



**HAL**  
open science

# Time-Division Multiplexing Architecture for Hybrid Filter Bank A/D converters

Davud Asemani, Jacques Oksman

► **To cite this version:**

Davud Asemani, Jacques Oksman. Time-Division Multiplexing Architecture for Hybrid Filter Bank A/D converters. 50th IEEE Midwest Symposium on Circuits and Systems, Aug 2007, Montréal, Canada. pp.405-408. hal-00261832

**HAL Id: hal-00261832**

**<https://hal-centralesupelec.archives-ouvertes.fr/hal-00261832>**

Submitted on 10 Mar 2008

**HAL** is a multi-disciplinary open access archive for the deposit and dissemination of scientific research documents, whether they are published or not. The documents may come from teaching and research institutions in France or abroad, or from public or private research centers.

L'archive ouverte pluridisciplinaire **HAL**, est destinée au dépôt et à la diffusion de documents scientifiques de niveau recherche, publiés ou non, émanant des établissements d'enseignement et de recherche français ou étrangers, des laboratoires publics ou privés.

# Time-Division Multiplexing Architecture for Hybrid Filter Bank A/D converters

Davud Asemami, Jacques Oksman

Department of Signal Processing and Electronic Systems  
 École Supérieure d'Électricité, 91192, Gif-sur-Yvette, France  
 Email: firstname.lastname@supelec.fr

**Abstract**—In this paper, a new Hybrid Filter Bank (HFB) architecture called Time-Division Multiplexing (TDM) is proposed for HFB-based A/D Converters (ADC). The TDM HFB architecture is firstly extracted considering the TDM components of analog input as new input vector. The TDM HFB-based ADC is then simulated using simply-realizable analysis filters to approve the mathematical formulation of the TDM model. At last, the output resolutions of TDM and classical HFB-based ADC are compared considering practical analog filters including realization errors. It is shown that the TDM architecture is less sensitive to the realization errors than the classical HFB. Besides, the TDM HFB can exploit a blind technique to correct the realization errors in opposite to the classical HFB case.

## I. INTRODUCTION

The flash (or all parallel) A/D Converters (ADCs) represent the most commonly used architecture for high speed A/D conversion. However, the complexity of flash ADC circuit grows exponentially with the number of bits of the resolution. In addition, it is exceedingly difficult to integrate analog part with a VLSI digital signal processor because of the large ADC die size and for process bandwidth requirements [1]. The demand for A/D or D/A converters with higher speeds has dramatically increased for realizing the new communications concepts such as Software-Defined Radio (SDR) approach [2]. The continuous-time HFB structure using analog analysis filters has been proposed as a suitable candidate for realizing the wide-band ADCs (Fig. 1) [3], [4]. Employing this parallel structure,  $M$  A/D converters are used in parallel working at  $\frac{1}{MT}$  whereas the original analog input is supposed to be limited to the frequency interval  $[-\frac{\pi}{T}, \frac{\pi}{T}]$ . An  $M$ -branch HFB-based ADC exhibits  $M - 1$  interference terms called *aliasing* at the output which restrict the output resolution like the quantization noise. The analog HFB-based A/D converters have exhibited a good performance (low aliasing terms) using simply-realizable first- and second-order analysis filters and FIR digital synthesis filters if a small ratio of oversampling is considered. However, the related performance in the presence of even small realization errors degrades so much [5]. It is then necessary to somehow correct the realization errors for having a useful HFB-based ADC. Digital techniques have been dealt with for managing the problem of high sensitivity to the realization errors. However, the proposed methods are limited to some specific errors or cases [6].

The blind deconvolution techniques can be employed as a candidate for handling the sensitivity of analog circuits to the

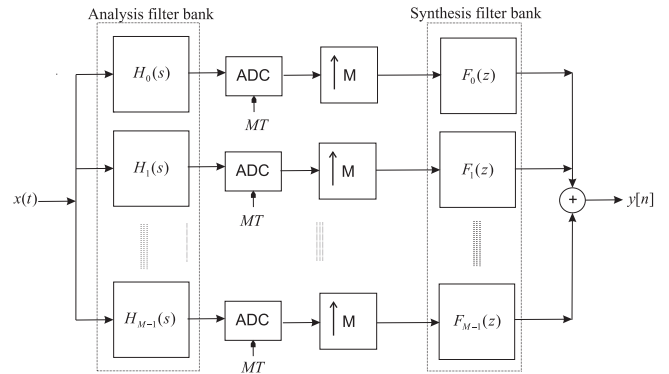


Fig. 1. The classical HFB-based A/D converter.

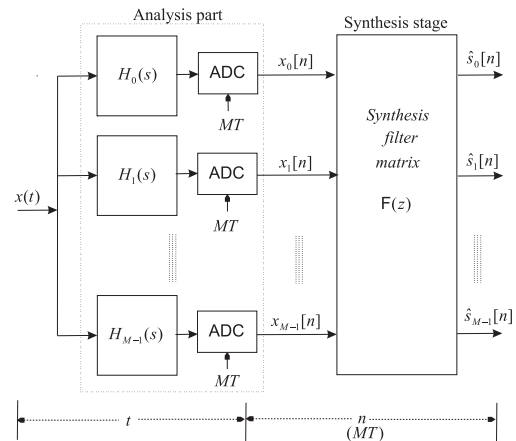


Fig. 2. The TDM architecture of HFB-based ADC. The outputs  $\hat{s}_0[n]$ ,  $\hat{s}_1[n]$ , ..., and  $\hat{s}_{M-1}[n]$  are the estimated TDM signals.

realization errors if the output of an LTI system is sampled at Nyquist (or a higher) rate [7]. Thus, the blind techniques can not be employed in the case of classical HFB architecture where an undersampling (at  $\frac{1}{MT}$ ) occurs at each branch. A new HFB structure called Time-Division Multiplexing (TDM) architecture is proposed in this paper (Fig. 2) to which blind deconvolution techniques can be applied. In the TDM HFB architecture,  $M$  consecutive samples (at the Nyquist rate  $\frac{1}{T}$ ) of the original input  $x(t)$  are supposed as the new input vector

$\mathbf{s}[n]$ :

$$\mathbf{s}[n] = \begin{bmatrix} s_0[n] \\ s_1[n] \\ \vdots \\ s_{M-1}[n] \end{bmatrix} = \begin{bmatrix} x(n'T) \\ x((n'-1)T) \\ \vdots \\ x((n'-(M-1))T) \end{bmatrix}_{n'=nM} \quad (1)$$

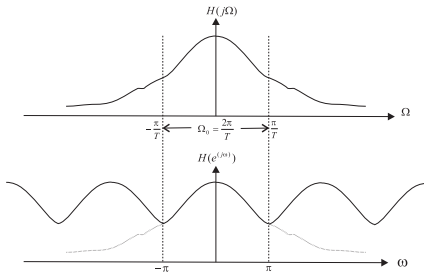
where  $n$  and  $n'$  may be supposed as the discrete-time indices associated with the sampling rates  $\frac{1}{MT}$  and  $\frac{1}{T}$  respectively. The TDM HFB-based ADC tries to approximate the input vector  $\mathbf{s}[n]$  at the output  $\hat{\mathbf{s}}[n]$ . For simplicity, the quantization noise is neglected throughout this paper [4]. The TDM HFB-based ADC is mathematically described and extracted in next section II. Then, considering the seven- and eight-branch HFBs, the TDM architecture is simulated to demonstrate the validity of proposed architecture in section III. Besides, the performance is compared between TDM and classical HFBs. At last, the characteristics of TDM HFB are summarized in conclusion.

## II. TDM ARCHITECTURE FOR HFB-BASED ADC

### A. Discrete-time model of analysis part

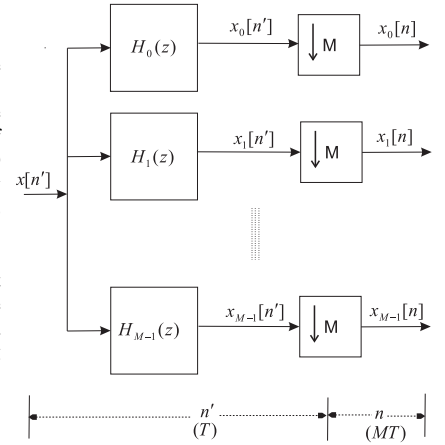
Without loss of generality, the classical HFB architecture is modeled in the discrete-time domain for conveniently extracting the new TDM architecture. According to Fig. 1, the input  $x(t)$  and analysis filters  $H_k(s)$  represent the only parameters which are not described in the discrete-time domain. Both of them belong to the analysis part of the HFB (see Fig. 2). The analog input  $x(t)$  may be sampled at  $\frac{1}{T}$  without any spectral overlapping because of Nyquist criterion. Then,  $x(t)$  can be replaced by  $x[n']$  in the discrete-time domain as  $x[n'] = x(n'T)$ . To obtain the equivalent  $H_k(e^{j\omega})$  of each analysis filter  $H_k(j\Omega)$ , Nyquist criterion can again be used (that the analog input  $X_k(j\Omega)$  is band-limited to  $\pm\frac{\pi}{T}$ ). Each  $H_k(j\Omega)$  may be substituted by a discrete-time filter  $H_k(e^{j\omega})$  obtained from periodically extending  $H_k(j\Omega)$  considering only the frequency interval of  $[-\frac{\pi}{T}, \frac{\pi}{T}]$  (refer to Fig. 3) [8]. If the

Fig. 3. Analog filter  $H(j\Omega)$  and its equivalent filter  $H(e^{j\omega})$  in the discrete-time domain for the HFB structure.



continuous-time components  $x(t)$  and  $H_k(j\Omega)$  are replaced by  $x[n']$  and  $H_k(e^{j\omega})$ , the samplers are eliminated and the discrete-time model of analysis part is obtained. This discrete-time model is shown in Fig. 4. Considering that model, the objective of HFB-based A/D conversion is to reconstruct the input  $x[n']$  at the output.

Fig. 4. The discrete-time model for the analysis part of HFB-based A/D converter. The only available signals are  $x_0[n]$ ,  $x_1[n]$ , ..., and  $x_{M-1}[n]$ .  $n'$  and  $n$  represent the discrete-time indices associated with the sampling rates  $\frac{1}{T}$  and  $\frac{1}{MT}$  respectively.



### B. TDM model of analysis part

The discrete-time model of analysis part (Fig. 4) is considered. To extract the TDM model of analysis part, the input signal  $x[n']$  is taken on parallel in the time-domain (refer to 1).  $\mathbf{s}[n]$  represents the new input vector. The Fourier transform  $S_k(e^{j\omega})$  of  $k^{th}$  TDM signal  $s_k[n]$  would be:

$$S_k(e^{j\omega}) = \frac{1}{M} e^{-j\frac{\omega}{M}k} \sum_{m=0}^{M-1} e^{j\frac{2\pi}{M}km} X(e^{j\frac{\omega}{M}-j\frac{2\pi}{M}m}) \quad (2)$$

Now, it is necessary to find a description for the outputs  $\mathbf{x}[n] = [x_0[n], x_1[n], \dots, x_{M-1}[n]]^T$  of analysis part in terms of  $\mathbf{s}[n]$ . Considering Fig. 4,  $x_k[n]$  can be described as:

$$\begin{aligned} x_k[n] &= \sum_{m=-\infty}^{\infty} h_k[m] x[n' - m] \Big|_{n'=Mn} \\ &= \sum_{r=0}^{M-1} \sum_l h_k[Mr + r] \cdot x[M(n-l) - r] \end{aligned} \quad (3)$$

To better reformulate 3,  $M$  intermediate digital filters  $h_{kr}[n]$  are defined in terms of the analysis filter  $h_k[n']$  as follows:

$$h_{kr}[n] = h_k[Mn + j] \quad 0 \leq r \leq M-1 \quad (4)$$

Using 1 and 4, the relationship 3 may be rewritten as:

$$x_k[n] = \sum_{r=0}^{M-1} \sum_l h_{kr}[l] \cdot s_r[n-l] = \sum_{r=0}^{M-1} h_{kr}[n] \star s_r[n] \quad (5)$$

where  $\star$  represents the convolution operation. Then, above relationship provides an LTI relationship between the available signals  $x_0[n]$ ,  $x_1[n]$ , ..., and  $x_{M-1}[n]$  (the outputs of analysis part) and the TDM input signals  $s_0[n]$ ,  $s_1[n]$ , ..., and  $s_{M-1}[n]$ . In the frequency domain, the digital filter  $h_{kr}[n]$  may be described as follows:

$$H_{kr}(e^{j\omega}) = \frac{1}{M} e^{j\frac{\omega}{M}r} \sum_{m=0}^{M-1} e^{-j\frac{2\pi}{M}rm} H_k(e^{j\frac{\omega}{M}-j\frac{2\pi}{M}m}) \quad (6)$$

Using equation 5, it can be shown in the matrix form that:

$$\mathbf{x}[n] = \mathbf{H}[n] \star \mathbf{s}[n] \quad (7)$$

where the vector  $\mathbf{x}[n]$  is:

$$\mathbf{x}[n] = \begin{bmatrix} x_0[n], x_1[n], \dots, x_{M-1}[n] \end{bmatrix}^T$$

$\mathbf{H}[n]$  represents an  $M \times M$  matrix whose  $(k, r)^{th}$  element is the impulse response of  $H_{kr}(e^{j\omega})$ . This LTI MIMO model can be described in the frequency domain as follows:

$$\mathbf{X}(e^{j\omega}) = \mathbf{H}(e^{j\omega})\mathbf{S}(e^{j\omega}) \quad (8)$$

Accordingly, an LTI MIMO model is obtained for the analysis part of HFB structure using the available  $\mathbf{x}[n]$  and TDM signals  $\mathbf{s}[n]$  as the output and input respectively. The TDM model of analysis part is illustrated in Fig. 5.

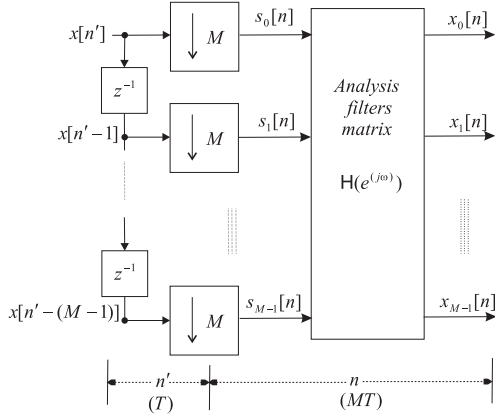


Fig. 5. Model of analysis part of HFB on the basis of TDM inputs.

### III. SIMULATING THE TDM HFB-BASED ADC

#### A. Design of synthesis stage

Considering the MIMO TDM model of analysis part (Fig. 5), a MIMO configuration for the HFB-based A/D converter may be obtained (Fig. 2). A matrix  $\mathbf{F}(e^{j\omega})$  of digital synthesis filters is used to reconstruct the input vector  $\mathbf{s}[n]$  of analysis filters matrix  $\mathbf{H}(e^{j\omega})$ . According to practical constraints, the analog analysis filters are firstly selected and fixed. Then, the synthesis filters  $\mathbf{F}(e^{j\omega})$  are realized by FIR digital filters since  $\mathbf{H}(e^{j\omega})$  is obtained from analog analysis filters (refer to 6). The frequency response  $\widehat{S}(e^{j\omega})$  of the output vector  $\widehat{\mathbf{s}}[n]$  (see Fig. 2) may be described in terms of the input vector  $S(e^{j\omega})$  as follows:

$$\widehat{S}(e^{j\omega}) = \mathbf{T}(e^{j\omega})S(e^{j\omega}) = \mathbf{F}(e^{j\omega})\mathbf{H}(e^{j\omega})S(e^{j\omega}) \quad (9)$$

where  $\mathbf{T}(e^{j\omega})$  is a matrix containing distortion and Inter-Channel Interference (ICI) terms. The estimated value  $\widehat{s}_k[n]$  of  $k^{th}$  TDM signal  $s_k[n]$  may be developed in the frequency domain as following:

$$\widehat{S}_k(e^{j\omega}) = \underbrace{T_{k,k}(e^{j\omega})S_k(e^{j\omega})}_{\text{Distortion term}} + \underbrace{\sum_{m=0, m \neq k}^{M-1} T_{k,m}(e^{j\omega})S_m(e^{j\omega})}_{\text{ICI terms}}$$

Fig. 6. Distortion and ICI terms of fourth TDM component  $s_3[n]$  in dB versus normalized frequency for a seven-branch HFB. The FIR synthesis filters consist of 64 coefficients.

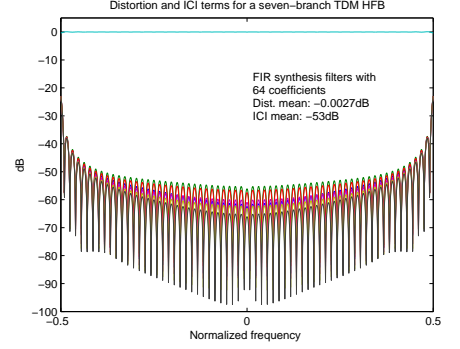
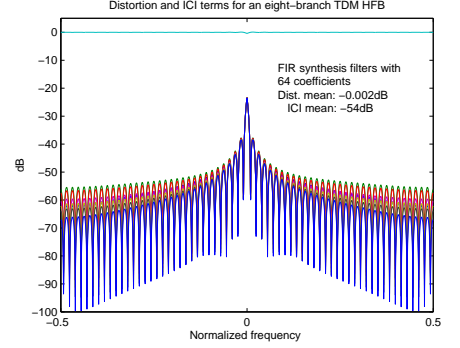


Fig. 7. Distortion and ICI terms of fourth TDM component  $s_3[n]$  in dB versus normalized frequency for an eight-branch HFB. The FIR synthesis filters include 64 coefficients.



$T_{kk}(e^{j\omega})$  stands for the distortion function related to the input component  $S_k(e^{j\omega})$ . The other  $M-1$  elements of  $(k)^{th}$  row of  $\mathbf{T}(e^{j\omega})$  represent the related ICI functions. The ICI elements are desired to be ideally null. Then, the Perfect Reconstruction (PR) equations at each frequency  $\omega$  will be:

$$\mathbf{F}(e^{j\omega})\mathbf{H}(e^{j\omega}) = \mathbf{I}e^{-j\omega n_d} \quad (10)$$

where  $\mathbf{I}$  represents the identity matrix ( $M \times M$ ) and  $n_d$  stands for an arbitrary delay.  $n_d$  is considered for maintaining the causality. Using PR equations, the frequency response of synthesis filters can be obtained at  $\omega$  as:

$$\mathbf{F}(e^{j\omega}) = e^{-j\omega n_d}\mathbf{H}^{-1}(e^{j\omega}) \quad (11)$$

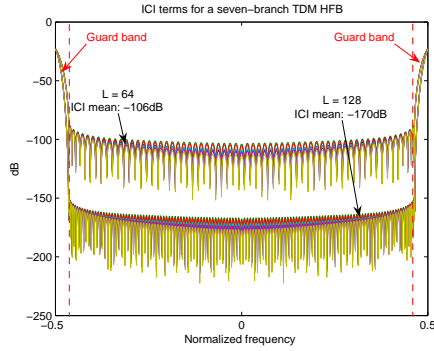
Having the frequency responses, the synthesis filters may then be approximated using FIR digital filters.

#### B. Simulation results

The analysis filter bank is supposed to include simply-realizable second-order RLC circuits except a first-order RC circuit as low-pass filter. The passing band of analysis filters are assumed to be constant. Considering seven- and eight-branch HFB structures ( $M = 7, 8$ ), the distortion and ICI terms related to the TDM signal  $s_3[n]$  are shown in Fig. 7 and 6 respectively. It may be seen that the ICI terms degrade around the frequencies of zero and  $\pm\pi$  for the even and odd number of branches respectively.

To improve the performance of TDM architecture, a Guard Band (GB) may be used at low or high frequencies depending on the number of branches. If the number  $M$  of branches

Fig. 8. ICI terms of fourth TDM component  $s_3[n]$  in dB versus normalized frequency for a seven-branch HFB. The FIR synthesis filters include 64 and 128 coefficients.



is odd, a percentage of the spectrum related to each TDM signal is allocated to the GB at the high frequencies. It means each TDM signal would be considered at the spectrum interval  $[-(1-\alpha)\pi, (1-\alpha)\pi]$  where  $\alpha$  represents the ratio of GB to the whole spectrum  $2\pi$ . In the even case, the GB is accommodated near the low frequencies. In other words, each TDM signal would include no information at the frequency interval  $[-\alpha\pi, \alpha\pi]$ . Fig. 8 exhibits the ICI terms related to the TDM signal  $s_3[n]$  of a seven-branch HFB considering a GB ratio of 7%. The FIR synthesis filters have 128 and 64 coefficients. To better show the performance improvement by using GB, table I provides the distortion and ICI mean values for the seven- and eight-branch TDM HFB structures considering 64 and 128 coefficients at each FIR synthesis filter. The performance has apparently improved by using a GB ratio of 7%. To compare the performance of TDM HFB

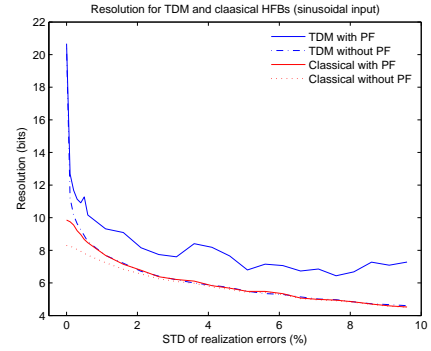
TABLE I

THE ICI AND DISTORTION AVERAGES FOR THE SEVEN- AND EIGHT-BRANCH TDM HFB STRUCTURES CONSIDERING  $L = 64$  AND  $L = 128$ .

Seven-branch TDM HFB (in dB)				
Guard band	0		7%	
$L$	ICI mean	Distortion	ICI mean	Distortion
64	-53.5	-0.0027	-106	-3.5E-10
128	-58.8	-0.0013	-169	2.1E-10
Eight-branch TDM HFB (in dB)				
Guard band	0		7%	
$L$	ICI mean	Distortion	ICI mean	Distortion
64	-54.1	-0.0023	-106	2.2E-7
128	-59.4	-0.0012	-170	2.5E-10

with the classical one, the output resolution of HFB structures is simulated in presence of realization errors. Applying a sinusoidal signal at the frequency  $\omega_o = \frac{0.5\pi}{8T}$  as the input, Fig. 9 shows the output resolution (in bits) of the classical and TDM HFBs versus the realization errors. An oversampling ratio of 7% is used for the classical HFB. If Post-Filtering (PF) is applied for eliminating the oversampling and GB spectral areas in the classical and TDM cases respectively, the TDM HFB architecture is associated with a performance of 3 bits better than the one related to the classical HFB in the presence of realization errors. It means that the TDM HFB is less sensitive than the classical one to the realization errors in the case of sinusoidal input. If GB spectral areas are not filtered

Fig. 9. The output resolution of the classical (in red) and TDM (in blue) HFB architectures versus the relative realization errors. A sinusoidal signal is the input. PF represents the Post-Filtering process.



out in the TDM HFB, it leads to the same resolution that a classical HFB may provide with eliminating the oversampling band. This shows that the TDM HFB architecture may provide at worst case (meaning without PF) the same performance as the classical one.

#### IV. CONCLUSION

A new HFB architecture called TDM is proposed for A/D conversion in this paper. The TDM HFB is mathematically described and the related design method is explained. Simulating the TDM HFB-based A/D converter, an acceptable performance in terms of ICI interferences is obtained if some percents of TDM components are allocated to GB. The output resolution of TDM HFB-based ADC is better than the classical one in the presence of realization errors of analysis filter bank. Besides, the TDM HFB architecture can exploit the blind techniques such as deconvolution for correcting the realization errors since the related inputs-outputs are associated by an LTI system without any decimation. In the classical HFB case, this is not possible because of undersampling process between the related input-output. The TDM HFB may be interesting for the Time-Division Multiple Access (TDMA) applications such as mobile communication systems.

#### REFERENCES

- [1] Abidi A. A., *Trends in high performance data conversion*, Int. Sym. on VLSI Technology, Systems, and Applications, pp.329-330, May, 1993.
- [2] Petraglia A. and Mitra S.K., *High-speed A/D conversion incorporating a QMF bank*, IEEE Transactions on Instrumentation and Measurement, vol. 41, no. 4, June, 1992, pp.427-431.
- [3] Velazques S.R., et al., *Design of Hybrid Filter Banks for A/D conversion*, IEEE Trans. on Sig. Processing, vol.46, nO.4, April, 1998, pp. 956-967.
- [4] Lowenborg P., et al., *Two-channel digital and hybrid Analog/Digital multirate filter banks with very low-complexity analysis or synthesis filters*, IEEE Transactions on Circuits and Systems, vol. 50, no. 7, July, 2003, pp.355-367.
- [5] Asemanni D. and Oksman J., *Influences of oversampling and analog imperfections on hybrid filter bank A/D converters*, IEEE Midwest Symp. on Circuits and Systems (MWSCAS), San Juan, PR, Aug., 2006.
- [6] Sanada Y. and Ikehara M., *Digital compensation scheme for coefficient errors of complex filter bank parallel A/D converter in low-IF receivers*, IEEE Vehicular Technology Conf., vol. 4, May, 2001, pp. 1680-1684.
- [7] Asemanni D., et al., *Digital estimation of analog imperfections using blind equalization*, European Signal Processing Conference (EUSIPCO), Sept. 4-8, 2006, Florence, Italy.
- [8] Asemanni D., Oksman J., *Performance of subband HFB-based A/D converter*, International Symposium on Signal Processing and its Applications (ISSPA), Feb. 12-15, 2007, Sharjah, UAE.